

## Communications

## Diastereoselectivity

GermanInternationalEdition:Edition: DOI:DOI: 10.100210.1002/ange./anie.201602962016029688

## Quantification of Stereochemical Communication in Metal–Organic Assemblies

Ana M. Castilla, Mark A. Miller, Jonathan R. Nitschke,\* and Maarten M. J. Smulders\*

**Abstract:** The derivation and application of a statistical mechanical model to quantify stereochemical communication in metal–organic assemblies is reported. The factors affecting the stereochemical communication within and between the metal stereocenters of the assemblies were experimentally studied by optical spectroscopy and analyzed in terms of a free energy penalty per “incorrect” amine enantiomer incorporated, and a free energy of coupling between stereocenters. These intra- and inter-vertex coupling constants are used to track the degree of stereochemical communication across a range of metal–organic assemblies (employing different ligands, peripheral amines, and metals); temperature-dependent equilibria between diastereomeric cages are also quantified. The model thus provides a unified understanding of the factors that shape the chirotopic void spaces enclosed by metal–organic container molecules.

By virtue of their hollow interiors, metal–organic container molecules<sup>[1]</sup> offer great potential for a range of applications,<sup>[2]</sup> including guest binding and separation, cavity-controlled catalysis, and stabilization of reactive intermediates. In contrast to the many enantioselective transformations catalyzed inside an enzyme’s (chiral) active site, in synthetic hosts the role of stereochemistry<sup>[3]</sup> has received little attention, with the focus mostly on controlling the size of the host cavity to steer guest binding or catalysis.<sup>[4]</sup> Reports addressing stereochemistry in metal–organic assemblies have so far mainly dealt with the synthesis of enantiopure cages,<sup>[5]</sup> (interconverting) diastereomeric species,<sup>[6]</sup> stereochemical switches,<sup>[7]</sup> enantioselective catalysis,<sup>[8]</sup> or guest binding.<sup>[9]</sup>

To emulate the enantioselectivity displayed by enzymes, insights into the conditions under which chiral ligands induce the formation of an enantiopure metal–organic self-assembled capsule are required. Such rules can guide the design of new container molecules offering enantioselective guest binding or catalysis, and may have implications for the understanding of the origin of biological homochirality.<sup>[10]</sup> A quantitative analysis based on statistical mechanics has proven useful in the description of chiral amplification in covalent and supramolecular polymers.<sup>[11]</sup>

The present work provides a quantitative description of the degree of stereochemical information transfer within discrete metal–organic cages. Building upon the pioneering work of Piguet on quantifying subtle thermodynamic effects in the self-assembly of polynuclear complexes,<sup>[12]</sup> we develop a simple statistical mechanical model that quantifies the effects of various factors, such as the choice of metal, chiral residue, ligand length, and temperature. We start with the phenomenon of amplification of stereochemical information as previously observed in a Fe<sup>II</sup><sub>4</sub>L<sub>6</sub> cage with a strong preference to have all metal centers with the same allD configuration.<sup>[13]</sup> We then examine this phenomenon in related tetrahedral cages with different metals, ligand lengths, or geometries (Figure 1). We also apply the model to the temperature-dependent diastereomer distributions in tetrahedral cages with weaker stereochemical coupling between metal centers.

Sergeant-and-soldiers experiments (Figure 1, top), involving the substitution of residues of achiral amine a within a racemic Fe<sup>II</sup><sub>4</sub>L<sub>6</sub> cage (2a; Figure 1, bottom) with increasing amounts of a more nucleophilic enantiopure amine (S)-b, resulted in the quantitative induction of a single stereochemical configuration at all Fe<sup>II</sup> centers before 100% (12 equiv) of the chiral amine was added, as monitored by the chiroptical response.<sup>[13]</sup> This effect was shown to be enhanced in the cage with respect to a related mononuclear complex (1a) as a result of stereochemical coupling between metal centers in the cage.

To devise a statistical model to quantify this effect, we separate the two ways in which stereochemical information can be amplified in multinuclear structures. First, at each metal center, intra-vertex amplification can manifest itself when fewer than three chiral amine residues suffice to quantitatively induce a single D or L stereoconfiguration. Second, inter-vertex communication: the mechanical connection between metal centers by rigid ligands allows stereochemical information to be relayed between vertices in the framework.<sup>[14]</sup> As a result, the configuration at one metal center can influence or even dictate

[\*] Dr. M. M. J. Smulders

Laboratory of Organic Chemistry, Wageningen University  
Stippeneng 4, 6708 WE Wageningen (The Netherlands)  
E-mail: maarten.smulders@wur.nlDr. A. M. Castilla, Prof. J. R. Nitschke  
Department of Chemistry, University of Cambridge  
Cambridge CB2 1EW (UK)  
E-mail: jrn34@cam.ac.ukDr. M. A. Miller  
Department of Chemistry, Durham University  
South Road, Durham DH1 3LE (UK)Supporting information and the ORCID identification number(s) for the author(s) of this article can be found under <http://dx.doi.org/10.1002/anie.201602968>.

© 2016 The Authors. Published by Wiley-VCH Verlag GmbH &amp; Co. KGaA. This is an open access article under the terms of the Creative Commons Attribution License, which permits use, distribution and reproduction in any medium, provided the original work is properly cited.



the configuration of its neighbors. The resulting model is a finite Ising system with

Wiley Online Library

© 2016 The Authors. Published by Wiley-VCH Verlag GmbH & Co. KGaA, Weinheim



## Communications



Figure 1. Top: Chiral induction through subcomponent substitution ( $R=H$  or a bridge within a connecting ligand). Bottom: Overview of the metal–organic assemblies studied herein.

quenched field disorder controlled by the distribution of chiral amines. Related models<sup>[15]</sup> have been used to describe the binding of ions to polyelectrolytes<sup>[15a,b]</sup> and cooperativity in supramolecular chemistry.<sup>[15c]</sup>

We consider first the case of a mononuclear  $ML_3$  complex which we treat as a two-state system with D and L states, where D is the preferred configuration for all (S)-chiral amines in this work.<sup>[13]</sup> Taking the D state as reference, an (S)amine attached to a L center incurs a free energy penalty, denoted  $f_1$ , in units of the thermal energy  $k_B T$  (where  $k_B$  is the Boltzmann constant). The  $f_1$  value quantifies the strength of coupling between carbon and metal stereocenters. We treat each amine in a given metal coordination sphere as acting independently, and we take the probability of substitution as equal for all amines in the system.

For tetrahedral cages, we treat each of the four metal centers as a two-state system, as in the mononuclear case. Now, however, there is also inter-vertex communication, as a result of the preference of a ligand to have the same stereoconfiguration at its two ends in a given structure. Taking the DD and LL states of a ligand as the reference, we quantify the inter-vertex stereochemical coupling through the parameter  $f_2$ , defined as the free energy of the DL and LD states, divided by  $k_B T$ . The total dimensionless free energy of a given tetrahedral complex is a multiple of  $f_1$  plus a multiple of  $f_2$  depending on the number and location of chiral amines, and the stereoconfiguration at each of its metal centers.

A Boltzmann-weighted average over all stereoconfigurations yields the overall fraction  $x_D$  of D centers in an equilibrium solution of the cages (see Section S3.1 in the Supporting Information). The value of  $x_D$  depends on the parameters  $f_1$  and  $f_2$ , providing a physical interpretation of the populations of D and L centers observed in experiments. For given values of  $f_1$  and  $f_2$ , the model predicts how the excess chirality (i.e. the relative excess of D over L metal centers) increases with the fraction ( $s$ ) of substituted amine. Plots of chiral excess as a function of  $s$  approach a limiting form as the  $f_1$  and  $f_2$  values become large, that is, the shape of the curve eventually becomes insensitive to the precise values of  $f_1$  and  $f_2$  (see Section S3.2).

We first apply the model to analyze sergent-and-soldiers experiments,<sup>[13]</sup> which started either with a racemic  $Fe^{II}L_3$  complex

Angew. Chem. Int. Ed. 2016, 55, 10616–10620

© 2016 The Authors. Published by Wiley-VCH Verlag GmbH & Co. KGaA, Weinheim

www.angewandte.org 10617

## Communications

and fitted curves have been renormalized to 1 at a chiral amine concentration of 100% (see Section S3.3). Values of  $f_1$  were obtained by least-squares fitting to data from experiments with

(1a), or with the racemic cage  $Fe^{II}_4L_6$  (2a), and to which different amounts of (S)-amine were added (see Section S2 in the Supporting Information). We examined three chiral amines, (S)-b,<sup>[13]</sup> (S)-c, and (S)-d<sup>[16]</sup> (Figure 1, bottom), to differentiate between the abilities of the amines to induce a single-metal stereochemical configuration, as expressed by the  $f_1$  value. Figure 2A shows how the excess chirality, as probed by circular dichroism, varied with the amount of added amine. In these plots,

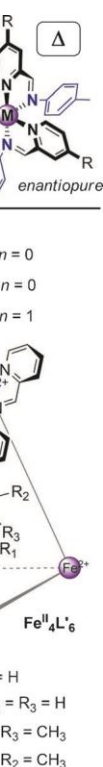
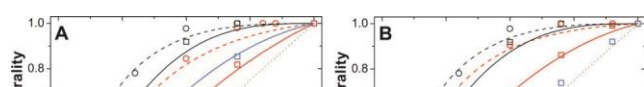


Figure 2. A–D) Sergent-and-soldiers sensitivity plots of excess chirality (experimental data points and fitted curves) versus added (S)amine. Plots in A) are for the addition of (S)-b, (S)-c, or (S)-d to  $Fe^{II}L_3$  or  $Fe^{II}_4L_6$  complexes (to form complexes 1b–d and 2b,c); B) show the addition of (S)-b to an  $ML_3$  or  $M_4L_6$  complex ( $M=Fe^{II}$ ,  $Co^{II}$ , or  $Zn^{II}$ ); C) show the addition of (S)-b to  $Fe^{II}L_3$ ,  $Fe^{II}_4L_6$ , and  $Fe^{II}_4L'_6$  complexes; D) show the addition of (S)-b to  $Co^{II}L_3$ ,  $Co^{II}_4L_6$ , and  $Co^{II}_4L_4$  complexes. E) Energy values for all complexes in MeCN (\*: value off-scale).



the  $Fe^{II}L_3$  complexes (Figure S1). These values were then fixed and used in a second fit to the experimental data obtained for the

related  $\text{Fe}^{\text{II}}_4\text{L}_6$  cages (Figure S4), to obtain an  $f_2$  value for each cage (Figure 2E).

The model accounts well for the shape of the experimental curves (Figure 2A). The  $f_1$  values of 38, 0.90, and 1.4 obtained for amines (S)-b, (S)-c, and (S)-d, respectively, highlight the much stronger ability of amine (S)-b than amine (S)-c in controlling the configuration at the metal center. The free energy penalty of 38 kJ/mol for (S)-b lies in the limiting regime of a large  $f_1$  value, where the sergeant-and-soldiers effect is overwhelming and the chiroptical response is insensitive to the exact value (Figure S8). Between (S)-c and (S)-d, (S)-d exhibited a stronger ability to control the configuration at the metal center, which we attribute to the greater bulk of the side group (cyclohexyl versus isopropyl).<sup>[16a,17]</sup> We infer that both sterics and  $\pi$ -stacking effects between phenyl and pyridyl rings are responsible for the strong influence of amine (S)-b upon the metal-centered configuration.<sup>[16a]</sup>

Using the  $f_1$  values from the  $\text{Fe}^{\text{II}}\text{L}_3$  complexes, experimental data could be fitted for the  $\text{Fe}^{\text{II}}_4\text{L}_6$  cages 2b and 2c; precipitation during the substitution of cage 2a with (S)-d precluded sergeant-and-soldiers studies with this amine. In these cages the  $\text{Fe}^{\text{II}}$  vertices are held together by the same ligand so similar  $f_2$  values are expected as  $f_2$  measures the ligand's ability to mediate stereochemical communication between the individual metal centers (as explained above). Gratifyingly, the values of  $f_2$  for cages 2b and 2c of 0.40 and 0.51, respectively, are similar. We attribute the small difference between the two values to uncertainty in fitting experimental data and to small differences in cage geometry as a result of the different amines.

Next, the effect of metal choice on the degree of amplification was studied by performing substitution experiments with (S)-b on the  $\text{Co}^{\text{II}}$  and  $\text{Zn}^{\text{II}}$ -containing analogues of the  $\text{Fe}^{\text{II}}\text{L}_3$  complex 1a (namely 3a and 4a) and the  $\text{Co}^{\text{II}}$ -templated analogue of the  $\text{Fe}^{\text{II}}_4\text{L}_6$  cage 2a (namely 5a; for each metal the chiroptical data were normalized at a different wavelength; Figure S3). Our model correctly predicts the sharp decrease in  $f_1$  value from 38 for  $\text{Fe}^{\text{II}}$ , to 1.3 for  $\text{Co}^{\text{II}}$  (3b), to approximately 0 for  $\text{Zn}^{\text{II}}$  (4b). Remarkably, no amplification was observed for  $\text{Zn}^{\text{II}}$ : the excess chirality of the  $\text{Zn}^{\text{II}}\text{L}_3$  complex 4b increased linearly as a function of added (S)-b. These observations can be understood in terms of the increased metal–ligand distance when going from  $\text{Fe}^{\text{II}}$  through  $\text{Co}^{\text{II}}$  to  $\text{Zn}^{\text{II}}$ ,<sup>[16a]</sup> with a concomitant reduction in bond strength (see Section S5 in the Supporting Information), which in turn decreases the steric gearing of the chiral amine residues required for effective stereochemical control around the metal center.

Despite similar  $f_2$  values, because of the smaller  $f_1$  value for  $\text{Co}^{\text{II}}$ , the enhancement in nonlinear effects in a  $\text{M}_4\text{L}_6$  cage with respect to a  $\text{ML}_3$  complex is more pronounced in the case of the  $\text{Co}^{\text{II}}$ -containing structures, 3b and 5b, than for their  $\text{Fe}^{\text{II}}$ -templated analogues 1b and 2b (Figure 2B). Because the  $\text{Zn}^{\text{II}}$ -analogue of 2a could not be prepared without an anionic template (see Section S1), its amplification behavior was not studied.

The effect of ligand structure on the degree of stereochemical communication within tetrahedral cages was studied by

examining the substitution with the same amine ((S)-b) of two other  $\text{Fe}^{\text{II}}$  cages: cage 6a,<sup>[18]</sup> built from a longer ditopic ligand (compared to 2a), and cage 7a, based upon a tritopic ligand.<sup>[16b]</sup> For cage 6b, the  $f_2$  value of 0.45 is only slightly higher than the value of 0.40 for 2b, verifying quantitatively the previous observation that linker length does not strongly affect the degree of stereochemical communication in these cages.<sup>[17a]</sup>

In stark contrast with the behavior of the  $\text{ML}_3$  complexes and  $\text{M}_4\text{L}_6$  cages studied, the substitution of the  $\text{Fe}^{\text{II}}_4\text{L}_4$  cage 7a with (S)-b was observed to occur through a cooperative imine exchange process (see Section S4), confirming the previously reported kinetic stability of this  $\text{Fe}^{\text{II}}_4\text{L}_4$  framework.<sup>[16b]</sup> Not being able to use cage 7a to investigate the degree of stereochemical coupling between metal centers in  $\text{M}_4\text{L}_4$  structures, we turned to its  $\text{Co}^{\text{II}}$ -containing congener (8a), which was not observed to undergo cooperative amine exchange (Figure S7, Figures S36–S37). For  $\text{Co}^{\text{II}}_4\text{L}_4$  cage 8b, stronger inter-vertex communication was observed, as expressed by an  $f_2$  parameter of 1.5, which is significantly higher than the value of 0.55 for the corresponding  $\text{Co}^{\text{II}}_4\text{L}_6$  cage 5b (Figure 2E). We infer that the tritopic ligands have a strong “gearing” effect within the rigid structure, forcing the four metal centers in the cage to adopt a homochirally pure D state. This strong inter-vertex stereochemical coupling has been shown to enable stereochemical memory in a  $\text{Fe}^{\text{II}}_4\text{L}_4$  cage.<sup>[16b]</sup>

In addition to analyzing the transmission of stereochemical information in all-D or all-L cages, we have also applied our model to a set of racemic  $\text{Fe}^{\text{II}}_4\text{L}_6$  cages (9–12; Figure 1) that have been previously observed to form heterochiral species.<sup>[6b]</sup> These assembled from ditopic achiral ligands (that is, with  $f_1=0$ ) based on terphenyl linkers with different methylation patterns. Cages 9–12 were found to exist in solution as an equilibrium between homochiral T (DDDD/LLLL), heterochiral  $\text{C}_3$  (DDDL/LLLD), and achiral  $\text{S}_4$  (DDLL) diastereomers. Moreover, variable-temperature NMR studies revealed these equilibria to be temperature-dependent.

The model can be employed to make a direct prediction of universal curves for the equilibrium distribution of the three diastereomers as a function of  $f_2$  value (Figure 3). We have placed the temperature-dependent distribution of diastereomers for cages 9–12 on these curves by finding the point on the  $f_2$  axis where each set of three yields fits best. There is no guarantee that an arbitrary set of three diastereomer fractions could be consistently placed on the curves. Hence, the observation that all data sets, apart from those for cage 9, can be superimposed on the plot provides strong support for the underlying model. The behavior of the four cages is very different. Cage 11 has strongly negative values for  $f^2$  ( $< -2$ ), indicating that the ligand prefers to connect two metal centers of opposite handedness, thus favoring the  $\text{S}_4$  diastereomer (wherein four of the six ligands link metal centers of opposite configuration). Cage 10 shows the opposite behavior: the

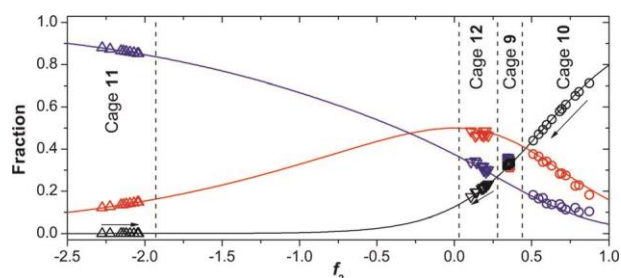


Figure 3. Experimental diastereomer distribution and predicted distribution as function of the  $f_2$  value (diastereomers: T=black;  $C_3$ =red;  $S_4$ =blue) for cage 9 (&), 10 (\*), 11 (-), and 12 (i). Arrows indicate increasing temperature.

homochiral T diastereomer is favored by the positive  $f_2$  value (about 0.9 at room temperature). However, raising the temperature decreases the  $f_2$  value, thereby increasing the proportions of the  $S_4$  and  $C_3$  diastereomers at the expense of the T diastereomer. For cage 12 the  $f_2$  value was found to be close to 0 (independent of the temperature), resulting in a nearly unbiased statistical distribution (which would be 1:4:3 for T: $C_3$ : $S_4$ ). For cage 9 some discrepancies between the data and the model were observed for the  $S_4$  and  $C_3$  diastereomers. However, its behavior can still be characterized by the moderately positive  $f_2$  value of 0.35 that slightly favors the T diastereomer.

The direction and sensitivity of the change in  $f_2$  value with respect to temperature are determined by the sign and magnitude of the enthalpic contribution to the free energy. The enthalpic and entropic components of  $f_2$  can be extracted by a Van't Hoff type analysis and can be shown by our model to relate to all three of the pairwise equilibria<sup>[6b]</sup> between the T,  $S_4$ , and  $C_3$  states (see Section S6 in the Supporting Information). The generally good agreement between the separately determined entropies and enthalpies and those derived from our model further validates the applicability of the model, providing a unifying understanding of the equilibria. Apart from the case of cage 9, we found that it is entropically favorable to have opposite stereoconfiguration at the two ends of each ligand, even when that combination is enthalpically unfavorable.

Our statistical mechanical model thus accounts for the specific nonlinear response of excess chirality in metal–organic tetrahedra due to stereochemical communication within the structures. For the first time for metal–organic cages, the effect of structural features on the degree of stereochemical communication has been quantified in terms of two energy parameters with clearly defined physical meanings, and an overarching description of the temperature-dependent equilibrium between diastereomeric cages has been provided. The general nature of the model allows for its extension to new cage geometries<sup>[19]</sup> and related structures, such as metal–organic frameworks.<sup>[20]</sup> We anticipate that the physical insight our model provides into the nuanced stereochemistry of the chirotopic cavities of these structures will translate into control over stereoselective guest binding and catalysis.<sup>[8b,9b]</sup>

## Acknowledgements

This work was supported by the European Research Council, the Netherlands Organization for Scientific Research (Veni Grant 722.012.005; to M.M.J.S.), and the Engineering and Physical Sciences Research Council (grant EP/I001352/1; to M.A.M.). We thank I. A. Riddell and S. Ma for providing ligands to prepare cages 2, 5, and 6, respectively.

**Keywords:** cage compounds · diastereoselectivity · statistical mechanics · stereochemical communication · supramolecular chemistry

How to cite: *Angew. Chem. Int. Ed.* 2016, 55, 10616–10620 *Angew. Chem.* 2016, 128, 10774–10778

- [1] T. R. Cook, P. J. Stang, *Chem. Rev.* 2015, 115, 7001.
- [2] a) M. Yoshizawa, J. K. Klosterman, M. Fujita, *Angew. Chem. Int. Ed.* 2009, 48, 3418; *Angew. Chem.* 2009, 121, 3470; b) M. Yamashina, Y. Sei, M. Akita, M. Yoshizawa, *Nat. Commun.* 2014, 5, 4662; c) R. Custelcean, *Chem. Soc. Rev.* 2014, 43, 1813; d) S. Lçffler, J. Libben, L. Krause, D. Stalke, B. Dittrich, G. H. Clever, *J. Am. Chem. Soc.* 2015, 137, 1060.
- [3] A. M. Castilla, W. J. Ramsay, J. R. Nitschke, *Acc. Chem. Res.* 2014, 47, 2063.
- [4] a) B. Olenyuk, M. D. Levin, J. A. Whiteford, J. E. Shield, P. J. Stang, *J. Am. Chem. Soc.* 1999, 121, 10434; b) J. Hamacek, D. Poggiali, S. Zebret, B. E. Aroussi, M. W. Schneider, M. Mastalerz, *Chem. Commun.* 2012, 48, 1281.
- [5] a) Z. R. Bell, J. C. Jeffery, J. A. McCleverty, M. D. Ward, *Angew. Chem. Int. Ed.* 2002, 41, 2515; *Angew. Chem.* 2002, 114, 2625; b) O. Chepelin, J. Ujma, X. Wu, A. M. Z. Slawin, M. B. Pitak, S. J. Coles, J. Michel, A. C. Jones, P. E. Barran, P. J. Lusby, *J. Am. Chem. Soc.* 2012, 134, 19334; c) R. Annunziata, M. Benaglia, M. Cinquini, F. Cozzi, C. R. Woods, J. S. Siegel, *Eur. J. Org. Chem.* 2001, 173; d) S. E. Howson, L. E. N. Allan, N. P. Chmel, G. J. Clarkson, R. van Gorkum, P. Scott, *Chem. Commun.* 2009, 1727; e) K. E. Jelfs, X. Wu, M. Schmidtmann, J. T. A. Jones, J. E. Warren, D. J. Adams, A. I. Cooper, *Angew. Chem. Int. Ed.* 2011, 50, 10653; *Angew. Chem.* 2011, 123, 10841; f) Y. Ye, T. R. Cook, S.-P. Wang, J. Wu, S. Li, P. J. Stang, *J. Am. Chem. Soc.* 2015, 137, 11896; g) P. Bonakdarzadeh, F. Pan, E. Kalenius, O. Jurc'ek, K. Rissanen, *Angew. Chem. Int. Ed.* 2015, 54, 14890; *Angew. Chem.* 2015, 127, 15103.
- [6] a) R. W. Saalfrank, H. Maid, A. Scheurer, R. Puchta, W. Bauer, *Eur. J. Inorg. Chem.* 2010, 2903; b) W. Meng, J. K. Clegg, J. D. Thoburn, J. R. Nitschke, *J. Am. Chem. Soc.* 2011, 133, 13652; c) S. P. Argent, T. Riis-Johannessen, J. C. Jeffery, L. P. Harding, M. D. Ward, *Chem. Commun.* 2005, 4647.
- [7] D. Ray, J. T. Foy, R. P. Hughes, I. Aprahamian, *Nat. Chem.* 2012, 4, 757.
- [8] a) C. J. Brown, R. G. Bergman, K. N. Raymond, *J. Am. Chem. Soc.* 2009, 131, 17530; b) C. Zhao, F. D. Toste, K. N. Raymond, R. G. Bergman, *J. Am. Chem. Soc.* 2014, 136, 14409; c) Y. Nishioka, T. Yamaguchi, M. Kawano, M. Fujita, *J. Am. Chem. Soc.* 2008, 130, 8160.
- [9] a) D. Fiedler, D. H. Leung, R. G. Bergman, K. N. Raymond, *J. Am. Chem. Soc.* 2004, 126, 3674; b) T. Liu, Y. Liu, W. Xuan, Y. Cui, *Angew. Chem. Int. Ed.* 2010, 49, 4121; *Angew. Chem.* 2010, 122, 4215; c) W. Xuan, M. Zhang, Y. Liu, Z. Chen, Y. Cui, *J. Am. Chem. Soc.* 2012, 134, 6904; d) L. Mart'inez-Rodr'iguez, N. A. G. Bandeira, C. Bo, A. W. Kleij, *Chem. Eur. J.* 2015, 21, 7144.
- [10] K. Soai, T. Kawasaki, A. Matsumoto, *Acc. Chem. Res.* 2014, 47, 3643.

## Communications

- [11] S. K. Jha, K. S. Cheon, M. M. Green, J. V. Selinger, *J. Am. Chem. Soc.* 1999, 121, 1665.
- [12] C. Piguet, *Chem. Commun.* 2010, 46, 6209.
- [13] N. Ousaka, J. K. Clegg, J. R. Nitschke, *Angew. Chem. Int. Ed.* 2012, 51, 1464; *Angew. Chem.* 2012, 124, 1493.
- [14] J. Clayden, M. Pickworth, L. H. Jones, *Chem. Commun.* 2009, 547.
- [15] a) M. Borkovec, G. J. M. Koper, C. Piguet, *Curr. Opin. Colloid Interface Sci.* 2006, 11, 280; b) G. Koper, M. Borkovec, *J. Phys. Chem. B* 2001, 105, 6666; c) G. Ercolani, L. Schiaffino, *Angew. Chem. Int. Ed.* 2011, 50, 1762; *Angew. Chem.* 2011, 123, 1800.
- [16] a) S. E. Howson, L. E. N. Allan, N. P. Chmel, G. J. Clarkson, R. J. Deeth, A. D. Faulkner, D. H. Simpson, P. Scott, *Dalton Trans.* 2011, 40, 10416; b) A. M. Castilla, N. Ousaka, R. A. Bilbeisi, E. Valeri, T. K. Ronson, J. R. Nitschke, *J. Am. Chem. Soc.* 2013, 135, 17999.
- [17] a) N. Ousaka, S. Grunder, A. M. Castilla, A. C. Whalley, J. F. Stoddart, J. R. Nitschke, *J. Am. Chem. Soc.* 2012, 134, 15528; b) E. A. Opsitnick, X. Jiang, A. N. Hollenbeck, D. Lee, *Eur. J. Org. Chem.* 2012, 708.
- [18] S. Ma, M. M. J. Smulders, Y. R. Hristova, J. K. Clegg, T. K. Ronson, S. Zarra, J. R. Nitschke, *J. Am. Chem. Soc.* 2013, 135, 5678.
- [19] a) C. Gitz, R. Hovorka, C. Klein, Q.-Q. Jiang, C. Bannwarth, M. Engeser, C. Schmuck, W. Assenmacher, W. Mader, F. Topic', K. Rissanen, S. Grimme, A. Lützen, *Angew. Chem. Int. Ed.* 2014, 53, 1693; *Angew. Chem.* 2014, 126, 1719; b) J.-F. Ayme, J. E. Beves, D. A. Leigh, R. T. McBurney, K. Rissanen, D. Schultz, *J. Am. Chem. Soc.* 2012, 134, 9488.
- [20] M. Yoon, R. Srirambalaji, K. Kim, *Chem. Rev.* 2012, 112, 1196.

Received: April 11, 2016

Revised: April 29, 2016

Published online: June 2, 2016

